# HIGH QE, LOW EMITTANCE, GREEN SENSITIVE FEL PHOTOCATHODES USING $K_2CSSB$*

T. Vecchione, J. Feng, W. Wan, H. A. Padmore, LBNL, Berkeley, CA 94720, U.S.A.
I. Ben-Zvi, T. Rao, J. Smedley, BNL, Upton, NY 11973, U.S.A.
D. H. Dowell, SLAC, Menlo Park, CA 94025, U.S.A.

*Abstract*

The bialkali-antimonide photoemissive material $K_2CsSb$ possesses properties that are well suited for photocathodes in accelerator applications. These include high quantum efficiency and low transverse emittance when illuminated by visible light, robustness in terms of sensitivity to water contamination and long lifetimes when operated under UHV conditions. The primary difficulty identified in producing $K_2CsSb$ photocathodes is in the minimization of surface roughness, a phenomenon that is believed to lead to increased emittance and therefore decreased performance.

## INTRODUCTION

The Next Generation Light Source (NGLS) is designed to be a MHz repetition rate free-electron laser (FEL) that is to be built at Lawrence Berkeley National Laboratory. The low frequency gun is resonant at 187 MHz, making it compatible with conventional LINAC technologies. One consequence of this is that the cavity is large and permits standard pumping techniques to achieve UHV conditions of $1\times10^{-11}$ torr or less. The result is that surface sensitive semiconductor photocathodes with high quantum efficiencies (QE) can be used, provided that they meet the FEL design specifications. These requirements are that the emittance be less than 1 μm / mm-rms beam size, that the QE be greater than 1% in the visible, and that the photocathode lifetime be on the order of weeks. Visible illumination was specified because of the need to have efficient transverse and longitudinal pulse shaping[1] and the desirability of using compact and efficient laser sources, such as fiber lasers. The goal of the research reported on in this paper is to provide photocathodes that satisfy all of these requirements and thereby address what has been identified as a key challenge for next generation accelerator based light sources[2]. Here we report on the QE, transverse emittance, robustness under laser illumination and lifetimes due to contaminant exposure that might be expected in an RF gun of $K_2CsSb$ photocathodes.

The bialkali-antimonide material $K_2CsSb$ was chosen for the development of NGLS photocathodes for several reasons, some of which were simply practical in nature. Although not as robust as metal photocathodes the fact that $K_2CsSb$ can be operated with high QE in the visible part of the spectrum means that the power required from an IR drive laser is reduced by 6 orders of magnitude from that needed for metals. It is noted that this advantage is not unique to $K_2CsSb$ alone. For instance, gallium-arsenide (GaAs:Cs:O) photocathodes also have high QE in the visible but are known to be exceptionally reactive and possess the detrimental flaw of having both fast and slow temporal response, making them inappropriate for the generation of fs electron pulses. Likewise, cesium-telluride ($Cs_2Te$) photocathodes are relatively robust and have high QE in the UV but because they are not photoemissive in the visible it was decided to forgo them initially. Other motivations for choosing $K_2CsSb$ were based on a long history of published work, much of which relating to photo-multiplier tube applications[3]. Since Sommer's original discovery[4] the production and characteristics of $K_2CsSb$ have been investigated by a number of different authors[5,6], the crystal structure of the $K_{1-x}Cs_xSb$ series of compounds has been determined[7] and more recently the electronic structure of $K_2CsSb$ has been calculated[8]. Most importantly work published by Dowell et al.[9] has already demonstrated that $K_2CsSb$ is in fact capable of sustaining high current densities when used inside of an RF photoinjector, albeit with relatively long pulses and large emittance. Unfortunately progress was limited due to vacuum issues associated with the gun itself. Nevertheless it sets a strong foundation on which to build our present research.

## EXPERIMENT

To create $K_2CsSb$ photocathodes, a deposition system was constructed consisting of three subsections – a deposition chamber, a diagnostic chamber, and a load lock allowing for cathode transfer and exchange. The deposition chamber is arranged such that light from a high brightness plasma source passes through a monochromator and a filter-wheel before being focused at normal incidence on the photocathode surface. The beam enters the deposition chamber through a fused silica viewport after passing a D-shaped mirror that is used to separate part of the beam for the purpose of flux monitoring. The optical system allows for sweeping in wavelength from 200-580 nm while recording the electron yield, producing Fowler scans of the photocathode. The deposited materials used to make the photocathodes are evaporated from low temperature Knudsen cells located symmetrically around the fused silica viewport. Antimony is evaporated from pure metal pellets while potassium and cesium are evaporated from dealloying sources that are purchased commercially (Bi-Cs and Bi-K; http://www.alvatec.com/).

* This work was supported by the Director of the Office of Science of the U. S. Department of Energy, under Contract No. DE-AC02-05CH11231, KC0407-ALSJNT-I0013, and DE-SC0005713.



ISBN 978-3-95450-117-5

A typical photocathode is produced by starting with an optically polished molybdenum substrate that is heat cleansed at 600 °C for 30 minutes prior to the deposition. Then a 200 Å layer of antimony is deposited with the substrate at a temperature of 160 °C. Following this potassium is evaporated at a substrate temperature of 140 °C until a maximum in the electron yield is observed. In the final step, cesium is deposited at a substrate temperature of 120 °C again until a maximum in the electron yield is observed. As shown in Fig. 1, the maximum QE reached is nominally 6% at 532 nm - which satisfies one of the photocathode design constraints for the NGLS.

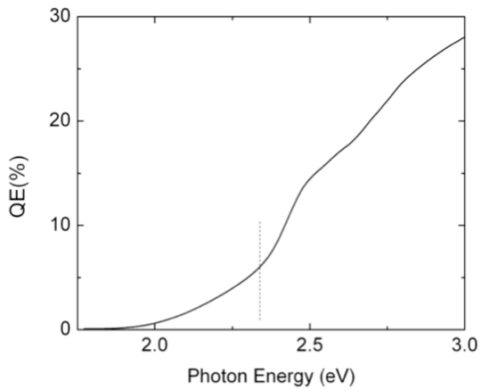


Figure 1: QE of $K_2CsSb$ at as a function of photon energy.

This performance has been replicated for both molybdenum and stainless steel substrates and using a range of different substrate temperatures in each step. It has also been replicated for multilayered depositions using varied ordering of the layers and co-depositions where all reactants are deposited simultaneously. Although the results are that different recipes produce cathodes with similar performance in terms of electron yield, these cathodes are not thought to be equal in terms of the emittance of the beams they generate, a topic that is discussed below.

Photocathodes formed using these methods can be stable over months when kept in ultra-high vacuum (UHV). They are also surprisingly stable to relatively high partial pressures of water. Fig. 2 shows the yield of a typical film as a function of time at a partial pressure of water of $5x10^{-9}$ torr recorded using 532 nm wavelength illumination. In this instance a 50% decay time of around 17 hours was found. As the partial pressure of water in DC, UHV low frequency RF and superconducting RF photo-guns is typically < $10^{-11}$ torr, the projected photocathode lifetimes given by residual vacuum conditions alone is thought to be sufficiently long. This satisfies another of the photocathode design constraints for the NGLS. Additionally, when illuminated with a green laser focused to a spot diameter of 100 µm, a current density of 100 mA/cm$^2$ has been verified without deterioration over the course of several days. This demonstrates photocathode robustness to Joule heating under static conditions.

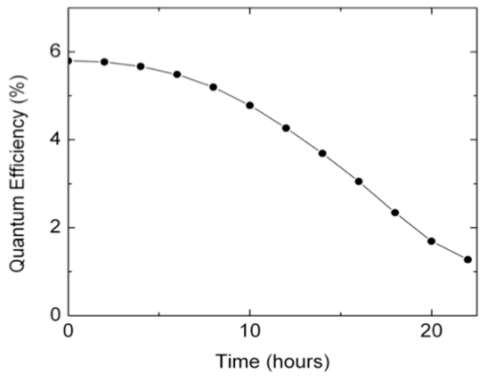


Figure 2: QE of $K_2CsSb$ as a function of time under 532 nm illumination with $5x10^{-10}$ torr partial pressure of $H_20$.

The diagnostic subsection of the deposition system is configured for making momentum distribution measurements and hence measuring the emittance of a beam generated at the photocathode. The experimental arrangement for this measurement is shown in Fig. 3. Here electrons are accelerated in a high gradient field of up to 3 MV/m generated between the photocathode and a mesh grid that are separated by a 5 mm gap. The extraction grid has a 25 µm mesh spacing and forms an immersion lens with a field free region that allows the beam to expand by drifting. The source of illumination can be any of 405, 473, 532, 543, 593 or 653 nm lasers focused on the photocathode at 30° through the grid, each with spot size of less than 200 µm FWHM. A lens coupled CCD camera images a phosphor screen located at the end of the drift region.

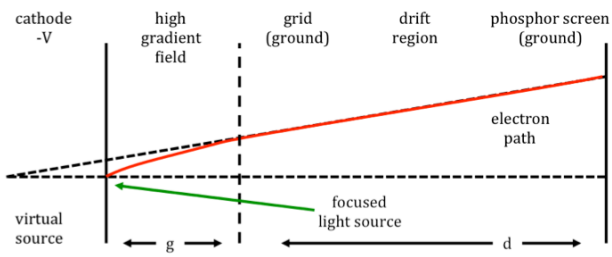


Figure 3: Experimental arrangement for measuring transverse momentum.

In this geometry we can relate the radial coordinate on the phosphor screen (r) and the normalized transverse momentum ($p_x$/mc) through,

$$r = \sqrt{\frac{mc^2}{2eV}}\left(2g + d\right)\left[\frac{p_x}{mc}\right] \qquad (1)$$

The term 2g + d indicates that electrons originate at a virtual source located a distance g behind the cathode as shown in Fig. 3. As configured, the system has an instrumental resolution that is less than kT resulting from the combination of two effects. The first is that each element of the grid acts as a diverging aperture lens[10]. This effect is small compared to the measured widths at



ISBN 978-3-95450-117-5

the phosphor screen for photocathodes with excess energies of less than a couple of volts. The second effect is that the mesh causes a sampling effect that leads to intensity modulations in the measured distribution. This effect is also small if the beam size is significantly larger than the mesh cell size. For further details the reader is referenced to a recent publication on using this method for measuring emittance[11].

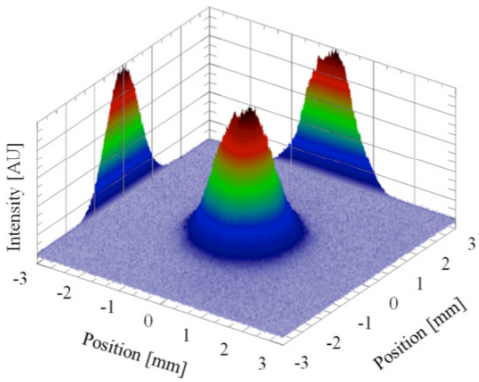


Figure 4: Image of the electron distribution of $K_2CsSb$ at 543 nm illumination with a 10 kV extraction potential.

Fig. 4 shows momentum distribution measurements of a $K_2CsSb$ cathode operated at 543 nm with a QE of 1%. From equation (1), and azimuthally integrating the intensity distribution we arrive at the radial distribution of normalized transverse momentum as shown in Fig. 5. This distribution can be used to calculate the normalized transverse emittance using,

$$\frac{\varepsilon_n}{\sigma_x} = \frac{\left\langle p_x^2 \right\rangle^{1/2}}{mc} \tag{2}$$

In this case the normalized transverse emittance was found to be 0.37 microns / mm-rms which is below the NGLS design requirement of 1 μm / mm-rms. Thus $K_2CsSb$ has been shown to be capable of satisfying each of the photocathode design constraints for the NGLS.

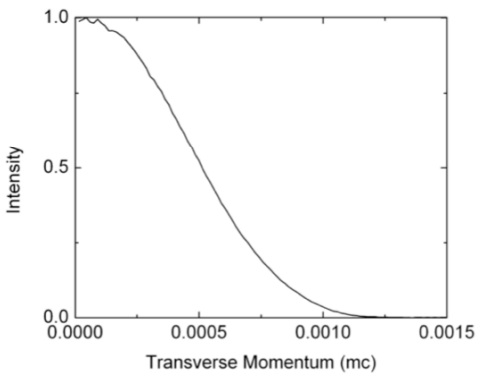


Figure 5: Transvserse momentum values following radial integration of the 2D distribution measured from $K_2CsSb$ at 543 nm light and 10 kV extraction potential.

Unfortunately simply measuring low emittance from $K_2CsSb$ does not conclude the overall evaluation. As stated earlier, not all photocathodes with equal QE are equal in terms of the emittance of the beams they produce. Figs. 5-6 illustrate this concept where the emittance of two different photocathodes is correlated to the thickness of the deposited film even though the QE is not. Data from a thin cathode is shown in Fig. 6 vs the equivalent data taken from a thicker cathode in Fig. 7. In all cases the emittance values measured for the thicker photocathode were significantly higher than for the thin one, e.g. at 532 nm the emittance grew from 0.43 to 0.57 μm / mm-rms beam size.

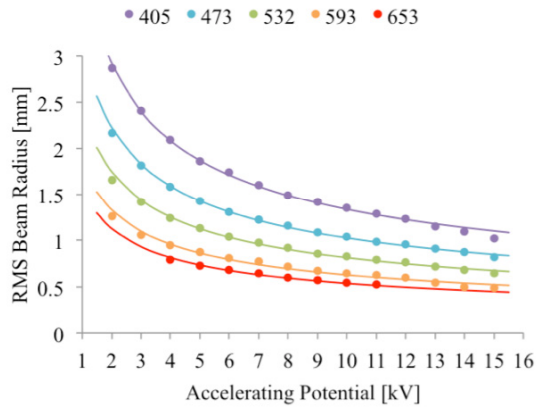


Figure 6: Beam radial RMS values corresponding to momentum distributions for a thin $K_2CsSb$ photocathode.

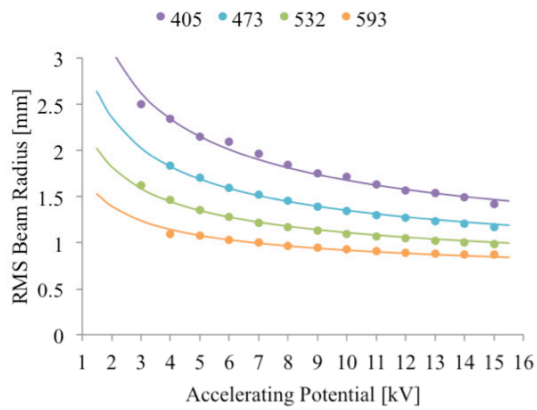


Figure 7: Beam radial RMS values corresponding to momentum distributions for a thicker $K_2CsSb$ photocathode.

It is our belief that the thicker film corresponds to larger grain sizes and therefore increased surface roughness. The increased surface roughness is thought to increase the intrinsic emittance of the beam produced. The rationale for this is that on average an electron is launched at an angle to the overall surface normal that is increased from what it would have been if the surface were indeed smooth, thereby increasing the emittance. In support of this we note that the expected variation in the

ISBN 978-3-95450-117-5

RMS beam size is proportional to $V^{-1/2}$ (V is the acceleration potential, Eqn. 1). This is indeed the case for the thin photocathode but is not the case for the thicker one, with a certain amount of offset making up the difference. Although our hypothesis is consistent with the measurements thus far, analysis is on-going. One difficulty encountered in verifying these results is due to the extreme reactivity of the surface when exposed to air – a necessary step in the current system for extracting photocathodes in order to measure surface roughness and absolute film thickness. In-situ techniques will need to be implemented in the immediate future in order to further support our hypothesis.

## CONCLUSIONS

In summary, we have shown that bialkali-antimonide $K_2CsSb$ possesses properties that are well suited for photocathodes used in accelerator applications. $K_2CsSb$ has a high quantum efficiency and low transverse emittance when illuminated by green light, robustness in terms of sensitivity to water contamination and long lifetimes when operated under UHV conditions. The primary difficulty we have identified in producing $K_2CsSb$ photocathodes is in the minimization of surface roughness, a phenomenon that is believed to lead to increased emittance and therefore decreased performance. In order to better characterize these effects we will be adding to the diagnostic section of the deposition system to provide for in-situ x-ray fluorescence and SEM imaging. The x-ray fluorescence will enable accurate measurements of elemental stoichiometry and the SEM imaging will permit us to observe any surface micro-roughness if present. Correlating these new measurements with the photocathode performance in terms of electron yield and emittance will be the focus of the next phase in our research. Following this, tests will be performed using a high fluence ps pulsed fiber laser to further demonstrate photocathode robustness. Once these steps have been completed the $K_2CsSb$ photocathodes will then begin testing inside the actual low frequency RF gun built for the NGLS.

## REFERENCES

[1] A. K. Sharma, T. Tsang, and T. Rao, Phys. Rev. ST Accel. Beams **12** (3), 033501 (2009).
[2] D. H. Dowell, I. Bazarov, B. Dunham et al., Nucl. Instrum. Methods **A622**, 685-697 (2010).
[3] A. H. Sommer, *Photoemissive Materials*. (John Wiley, 1968).
[4] A. H. Sommer, Applied Physics Letters **3** (4), 62-63 (1963).
[5] C. Ghosh and B. P. Varma, Journal of Applied Physics **49** (8), 4549-4553 (1978).
[6] A. di Bona, F. Sabary, S. Joly et al., Nucl. Instrum. Methods **A385** (3), 385-390 (1997).
[7] W. H. McCarroll, Journal of Physics and Chemistry of Solids **26** (1), 191-195 (1965).
[8] A. R. H. F. Ettema and R. A. de Groot, Physical Review B **66** (11), 115102 (2002).
[9] D. H. Dowell, S. Z. Bethel, and K. D. Friddell, Nucl. Inst. Meth. **356** (2-3), 167-176 (1995).
[10] C. J. Davisson and C. J. Calbick, Physical Review **42** (4), 580 (1932).
[11] T. Vecchione et al., Applied Physics Letters **99**, 034103 (2011).



ISBN 978-3-95450-117-5